Nuclear data study for Accelerator Driven System at J-PARC

Shin-ichiro MEIGO[†1]

[1]J-PARC Center, Japan Atomic Energy Agency, Shirakata 2-4, Tokai, Ibaraki, 319-1195, Japan
[†]Email: meigo.shinichiro@jaea.go.jp

To decrease the toxic waste produced at the nuclear reactor, studies of the Accelerator Driven System (ADS) are developing worldwide. Since the neutron production target at ADS is designed to be irradiated by protons in several GeV kinetic energy, a study with the high-energy particles in the kinetic energy region around GeV is essential for the research and development of ADS. However, many accelerator facilities using several GeV-protons built in the 1970s have been shut down due to their lifetime. Eventually, the facilities to be able to use protons with several GeV are scarce in the world. In Japan, J-PARC can only apply for the sake of ADS using the hadron, including proton. Using the 3-GeV proton synchrotron, some studies are going at J-PARC aimed at obtaining the nuclear data of ADS. In this paper, some experiment results related to nuclear data for ADS are introduced, such as nuclide production cross section induced by proton and displacement cross section.

1 Introduction

To reduce the hazards associated with the radioactive waste produced in a nuclear reactor, Japan Atomic Energy Agency (JAEA) proposed an accelerator-driven system (ADS) that comprises extremely high-power accelerators (30 MW) with proton kinetic energy of 1.5 GeV [1]. Since the neutron production target at ADS is designed to be irradiated by protons in several GeV kinetic energy, a study with the high-energy particles in the kinetic energy region around GeV is essential for the research and development of ADS. However, many accelerator facilities using several GeV-protons, such as SATURNE at CEA, established for nuclear physics in the 1970s, have been shut down due to their lifetime. Eventually, the facilities to be able to use protons with several GeV, such as AGS at BNL, PS at CERN, and U-10 at ITEP, are scarce in the world. In Japan, J-PARC can only apply for the sake of ADS using the hadron, including proton. Therefore, our group conducted nuclear data studies for ADS at the 3-GeV proton synchrotron (RCS) facility and the beam transport line.

In this paper, some experiment carried out at J-PARC for the nuclear data for ADS using several GeV-protons are introduced, such as nuclide production cross section induced by protons [2, 3] and displacement cross section [4, 5].

2 Displacement cross section

In ADS, Lead–bismuth eutectic (LBE) is used as a target material, and it simultaneously plays the role of a coolant. While designing ADS, damage to the beam-intercepting material is one of

the critical issues. In other high-intensity accelerator facilities, the beam–intercepting material also plays essential roles. To confidently operate a high-power accelerator, damage estimation of the target material is essential. For quantitative specification of the damage to the target material, the displacement per atom (dpa) index is generally employed. A dpa is widely used for the estimation of the damages caused to nuclear reactors and fusion reactors. The dpa is estimated using the particle fluence multiplied with displacement cross section. The cross section is usually obtained using the Norgertt–Robinson–Torrens (NRT) model [6]. In the low-energy region below 20 MeV, the displacement cross section for a proton can be reliably predicted because the Coulomb force mainly causes the displacement. The calculation method for the displacement cross section has been established for the low-energy regions where nuclear reactions produce no particles. However, for the protons in the high-energy region above 20 MeV, the experimental data of the displacement cross section are scarce. Therefore, the displacement cross section has not been adequately studied. Since many reaction channels open (above 20 MeV), calculation codes based on the intra-nuclear cascade model are used to obtain the cross section. Although iron materials play essential roles, such as the beam window for the ADS and target vessels of the spallation neutron source, the experimental data of the displacement cross section have not been observed in the energy region above 20 MeV. For validation and improvement of the dpa evaluation, the experimental data are crucial.

2.1 Experiment of displacement cross section

For the displacement cross-section measurement, we conducted experiments at 3-GeV proton beam transport (3NBT) line at the J-PARC. A vacuum chamber with a cryocooler was installed at the front of the beam dump of the 3-GeV rapid cycling synchrotron (RCS). At the RCS, the kinetic energy of the extracted proton can vary from 0.4 to 3 GeV, altering the timing of the extraction kicker magnet. With the change in the rigidity of the following magnets, the beam was introduced to the sample.

Since there was no space in the beamline introduced to the beam dump, the present experiment equipment was installed in the beamline, where the high-intensity proton beam could be delivered to the spallation neutron source in the MLF. Although the low-intensity proton beam was irradiated to sustain the cryogenic temperature of the sample, an additional interlock of the accelerator was required for the experiment owing to safety reasons, which changed the licensing of the RCS described in Japanese law of act concerning prevention from radiation hazards due to radioisotopes.

At the RCS, the kinetic energy of the extracted proton can vary from 0.4 to 3 GeV, altering the timing of the extraction kicker magnet. With the change in the rigidity of the following magnets, the beam was introduced to the sample. For observation of the damage in the sample, the irradiated sample is required to be cooled at a cryogenic temperature (around 10 K), where the recombination of Frenkel pairs is well suppressed owing to thermal motion. With the observation of the resistivity change $\Delta\rho$ due to the irradiation at the cryogenic temperature, the experimental displacement cross section $\sigma_{exp}(E)$, is given by the following,

$$\sigma_{exp}(E) = \Delta\rho/(\overline{\phi(E)}\rho_{FP}), \tag{1}$$

where $\overline{\phi(E)}$ is the average proton fluence at the sample over irradiation time, ρ_{FP} is the resistivity change per Frenkel-pair density for a particular metal, which has an uncertainty of 20%.

A vacuum chamber was installed in front of the 3-GeV beam dump. The chamber that was installed at the beam transport line maintained vacuum pressure less than 10^{-5} Pa using the sputter-ion pumps. The chamber was equipped with a Gifford–McMahon (GM) (Sumitomo Heavy Industries RDK-408D2) cryocooler. The GM cryocooler cooled the sample using an

oxygen-free high-conductivity copper rod and sample holder made of aluminum that was placed at the tip of the copper rod, as shown in **Fig. 1**. The GM cooler comprises two structures: the 1 st and 2 nd stages. At the 1 st and 2 nd stages, the temperatures can reach 40 K and 4 K, respectively. For the measurement of the thermal recovery of the sample, a heater was attached to the copper rod. The assembly of the GM cryocooler and a sample wire was placed on a movable stage to control the irradiation. Since the RCS kicks the beam horizontally for the extraction, the stability of the beam position in the vertical direction is better than in the horizontal.

To obtain the beam window material data used at the ADS, we selected iron as the sample. Before installation, the sample was annealed just less than the melting point to eliminate the defect of the lattice. Each sample was sandwiched between electrical insulation sheets of an aluminum nitride ceramic and held by the holder made of aluminum. To minimize the beam interaction on the holder, we made an aperture with 40-mm diameter for the sample holder. The resistance of the sample was measured using a voltmeter and current source. The sample wire was connected through terminals to both the current source and voltmeter for the compensation of the cable resistance between the sample and instruments. The precision of this resistance measurement was ± 0.01 $\mu\Omega$, corresponding to a resistivity of ± 3 fΩm.

The resistance thermometer on the sample holder was calibrated in the temperature range of 4 –100 K, and a silicon thermometer on the copper column was calibrated between 4 K and the room temperature. The resistance decreased with the temperature. It was observed that the resistance was saturated around the cryogenic temperature ($\sim$4 K).

The electrical resistivity of the sample ρ is expressed as follows: $\rho = RA/L$, where R [Ω] is the measured electrical resistance, A is the area of the sample (4.9×10^{-8} m^2) with a diameter of 250 μm, and L is the length between two potential points (40 mm). To avoid heat introduction to the sample owing to radiation to the sample, the sample was surrounded using double-walled radiation thermal shields made of aluminum. The outer and inner shields with a thickness of 2 and 1 mm, were directly connected to the1 st and 2 nd stage of the GM cooler, respectively. To minimize the scattering of the proton beam on the shields, we placed thin aluminum foils with a thickness of 5 μm and at the beam entrance and exit holes (with a diameter of 40 mm) for both thermal shields. After 6 h of cooling, the temperature of the sample holder was less than 4 K. Note that, in the early period of the experiment, the temperature was not 4 K, but $\sim$20 K. With some trials changing the conditions, the heat was introduced through the measurement cables for the resistance and temperature.

To fit the beam position on the sample precisely, the beam was vertically scanned with the steering magnet placed upstream of the sample along the beam direction. With the observation of the change in resistivity during the scan, the beam position given by the profile monitor was confirmed to be the center of the wire owing to the precious beam control developed at J-PARC [7, 8]. During the beam irradiation, the resistance of the iron sample was observed with the temperature of the sample holder determined using the attached thermometer. Although the sample temperature was not directly observed, it can be expected to be $\sim$4 K. During the irradiation of the sample, the temperature slightly increased. The observed temperature of the holder increased by 0.2 K. After irradiation, the sample resistance was increased by about 0.2 $\mu\Omega$ from the start of the beam irradiation, which was produced due to the displacement.

2.2 Results of displacement cross section

Using Eq(1), the displacement cross sections of iron are obtained. In this work, the resistivity change per Frenkel-pair ρ_{FP} was defined as 2.46×10^{-6} $\pm$ 0.57 Ωm for iron, obtained from another study [9]. It should be mentioned that the error of the present cross-section data was dominated by the one of the resistivity change per Frankel-pair. To obtain high-precision results,

the uncertainties of the resistivity change by Frankel-pair creation need to be improved, which is expected to be achieved using an electron beam.

Figure 2 shows the calculation using PHITS [10] using cascade model of INCL-4.6 [11]. In **Fig. 2**, the evaluated data were given by the Karlsruhe Institute of Technology (KIT) [12]. For both calculated values, two models of NRT, which is widely utilized for evaluation of dpa, and the athermal–recombination–corrected dpa (arc-dpa) model based on molecular dynamics (MD) were applied. The parameters given by Nordlund [13] was applied to PHITS. KIT used the binary collisional approximation (arc-dpa-BCA) model for evaluation. The displacement cross section of iron compared with the previous experimental data is shown in **Fig. 2**, in which the calculation by PHITS and the data evaluated by KIT [12] with the NRT and the arc-dpa models are also shown. The current data were found to be lower than the calculation with the NRT model with PHITS and KIT evaluation by about 2 times. On the other hand, the arc-model calculation showed remarkably good agreement with the experimental data.

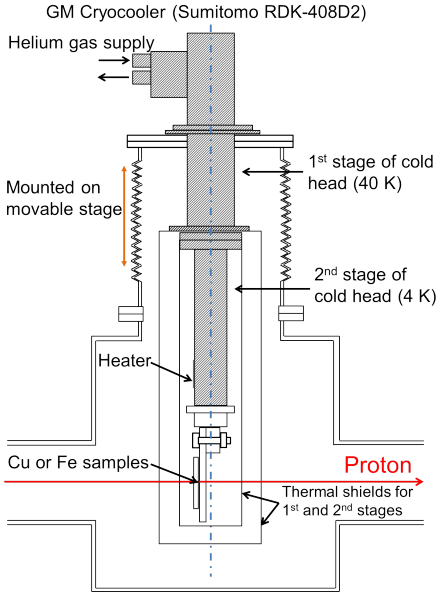

Figure 1: Schematic of the sample, vacuum chamber, and GM cryocooler used for the present experiment.

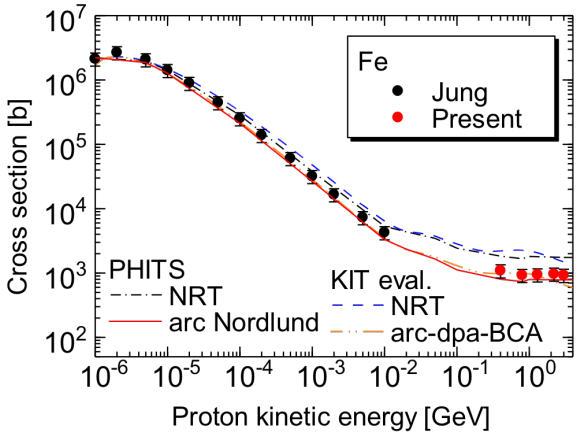

Figure 2: Comparison of the present experimental data for iron with previous experimental data [14], calculation data using PHITS [10] and KIT evaluations [12].

3 Production cross section induced by several GeV-protons

To estimate the residual nuclei in the beam window and the target, the production cross section is required. However, the data are not enough to validate the calculation models. For validation of the calculation model, we have been carried out the production cross section using several GeV-protons. For the experiment, sample changers with sample holders were installed at 3NBT. After irradiation, the sample was observed by the high-pure Germanium detector. With the gamma spectrometry, the production cross section was derived.

As an example, the experimental results of ^{nat}Fe(p,x)^{7}Be is shown in **Fig. 3** compared with the various calculation models and the evaluation data of JENDL-2007. It is shown that INCL++/ABLA07 and INCL/GEM show remarkable underestimation for the kinetic energy range above 1 GeV region. The nuclide of ^{7}Be is mainly produced by the statistical decay

and partially produced by the multifragmentation. On the other hand, the previous calculation model of Bertini/GEM shows good agreement in the energy range above 2 GeV. Although JENDL/HE-2007 shows a good agreement with the experimental results, it shows a slight overestimation for energies above 2 GeV. Using the present experimental results, the evaluation will be improved.

Just the same cross section for ^{56}Fe was measured by the GSI using the inverse-kinematics method, which is also shown in **Fig. 3**. The present data disagree the data observed at the GSI data [], which is pointed out by the other study [16]. It can be concluded that another study using inverse kinematics has worth to reveal the detailed production process for the improvement of the model.

4 Summary

To evaluate the target materials used in high-intensity proton accelerators, particularly in ADS, experiments for displacement and nuclei production cross-sections measurements were carried out in J-PARC. The displacement cross section of iron irradiated using protons having kinetic energies in the range 0.4 and 3 GeV was successfully obtained. It should be mentioned that the present data for iron is the first experimental data in the projectile energy region above 400 MeV, which is essential for the research and development of ADS. The present experimental data of the displacement cross sections were compared with the calculation using the PHITS and the data evaluated by KIT. The present results showed an overestimation of the cross section using the widely employed NRT model by a factor of 2∼3.5 based on the previous experiments, this model was preferred for the proton projectile with lower energy than 10 MeV. In contrast, the arc-dpa model shows remarkably good agreement with the present data. For the nuclei production cross section induced by several GeV-protons, further improvements to the model are required to reproduce the cross section. For this sake, we will continue the experiment at J-PARC.

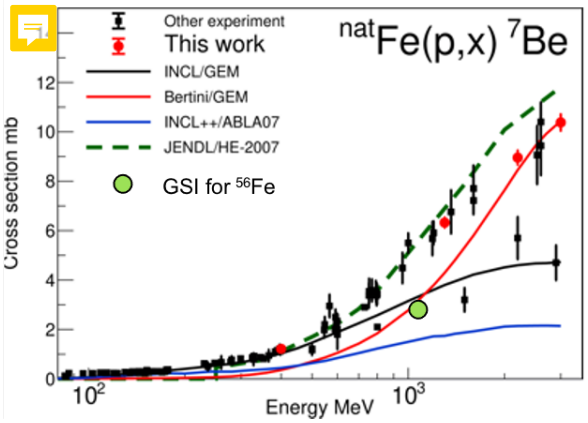

Figure 3: Production cross section of ^{nat}Fe(p,x)^{7}Be as a function of kinetic energy of projectile protons.

Acknowledgment

This paper partially contains the results of “Measurement of displacement cross section at J-PARC for structural material utilized at ADS” entrusted to JAEA by the Ministry of Education, Culture, Sports, Science, and Technology of Japan.

References

[1] Tsujimoto K, Oigawa H, Ouchi N, et al. Research and development program on accelerator driven subcritical system in JAEA. Journal of Nuclear Science and Technology. 2007; 44(3):483–490.

[2] Matsuda H, Meigo S, Iwamoto H. Proton-induced activation cross section measurement for aluminum with proton energy range from 0.4 to 3 GeV at J-PARC. Journal of Nuclear Science and Technology. 2018;55(8):955–961.

[3] Meigo S, Nishikawa M, Iwamoto H, et al. Measurement of aluminum activation cross section and gas production cross section for 0.4 and 3-gev protons. EPJ Web Conf. 2017;146:11039.

[4] Meigo S, Matsuda H, Iwamoto Y, et al. Measurement of Displacement Cross Section of Structural Materials Utilized in the Proton Accelerator Facilities with the Kinematic Energy above 400 MeV; 2020.

[5] Matsuda H, Meigo S, Iwamoto Y, et al. Measurement of displacement cross-sections of copper and iron for proton with kinetic energies in the range 0.4 – 3 GeV. Journal of Nuclear Science and Technology. 2020;57(10):1141–1151.

[6] Norgett M, Robinson M, Torrens I. A proposed method of calculating displacement dose rates. Nuclear Engineering and Design. 1975;33(1):50 – 54.

[7] Meigo S, Ohi M, Kai T, et al. Beam commissioning for neutron and muon facility at J-PARC. Nuclear Instruments and Methods in Physics Research Section A: Accelerators, Spectrometers, Detectors and Associated Equipment. 2009;600(1):41 – 43.

[8] Meigo S, Ooi M, Fujimori H. Two-parameter model for optimizing target beam distribution with an octupole magnet. Phys Rev Accel Beams. 2020 Jun;23:062802.

[9] Broeders C, Konobeyev A. Defect production efficiency in metals under neutron irradiation. Journal of Nuclear Materials. 2004;328(2):197 – 214.

[10] Iwamoto Y, Niita K, Sawai T, et al. Improvement of radiation damage calculation in PHITS and tests for copper and tungsten irradiated with protons and heavy-ions over a wide energy range. Nuclear Instruments and Methods in Physics Research Section B: Beam Interactions with Materials and Atoms. 2012;274:57 – 64.

[11] Boudard A, Cugnon J, David JC, et al. New potentialities of the liège intranuclear cascade model for reactions induced by nucleons and light charged particles. Phys Rev C. 2013 Jan; 87:014606.

[12] Konobeyev A, Fischer U, Simakov S. Improved atomic displacement cross-sections for proton irradiation of aluminium, iron, copper, and tungsten at energies up to 10 GeV. Nuclear Instruments and Methods in Physics Research Section B: Beam Interactions with Materials and Atoms. 2018;431:55 – 58.

[13] Nordlund K, Zinkle SJ, Sand AE, et al. Improving atomic displacement and replacement calculations with physically realistic damage models. Nature Communications. 2018;9(1):1084.

[14] Jung P. Atomic displacement functions of cubic metals. Journal of Nuclear Materials. 1983; 117:70 – 77.

[15] Napolitani P, Schmidt KH, Botvina AS, et al. High-resolution velocity measurements on fully identified light nuclides produced in ^{56}Fe + and ^{56}Fe+titanium systems. Phys Rev C. 2004 Nov;70:054607.

[16] Titarenko YE, Batyaev VF, Titarenko AY, et al. Cross sections for nuclide production in a ^{56}Fe target irradiated by 300, 500, 750, 1000, 1500, and 2600 mev protons compared with data on a hydrogen target irradiated by 300, 500, 750, 1000, and 1500 mev/nucleon ^{56}Fe ions. Phys Rev C. 2008 Sep;78:034615.